Photon emission from a single-molecule source driven by an rf field

Igor Rozhkov and E. Barkai
Department of Chemistry and Biochemistry, Notre Dame University, Notre Dame, Indiana 46556, USA
(Received 15 September 2004; published 18 March 2005)

The behavior of a single molecule driven simultaneously by a laser and by an electric radio frequency field is investigated using a non-Hermitian Hamiltonian approach. Employing the renormalization group method for differential equations, we calculate the average waiting time for the first photon emission event to occur, and determine the conditions for the suppression and enhancement of photon emission. An abrupt transition from localizationlike behavior to delocalization behavior is found.

DOI: 10.1103/PhysRevA.71.033810 PACS number(s): 42.50.Ar, 31.15.−p, 33.80.−b

Periodic driving of a two-level system can significantly alter its dynamics. Two renowned examples are dynamical localization of ultracold atoms in magneto-optical traps [1], and coherent destruction of tunneling (CDT) for a particle (e.g., an electron) in a bistable system [2]. In the latter example, a sinusoidal external driving field localizes the electron in one of the wells of a double-well potential. This is done via particular choice of parameters of the driving field [2]. Such a coherent localization behavior was recently addressed in Ref. [3] in the context of single-molecule spectroscopy [4].

When a molecule interacts with a continuous wave laser field and a much slower radio frequency (rf) field, one can control the emission of the molecule by the appropriate selection of the rf field parameters (see Ref. [3]). Coherent localization in this case manifests itself as the divergence of average waiting time for a single-photon emission, even when the laser frequency is in resonance with the electronic absorption frequency of the molecule. The rf field effectively localizes the wave function of the molecule in its ground state (i.e., for certain special parameters of the rf driving field). Note that control of emission by single molecules using rf fields has gained interest recently since it can be used for single-photon control and hence, possibly for quantum cryptology and quantum computing [4,5].

In this paper we present the criterion for the destruction and enhancement of emission from a single-molecule source interacting with an on-resonance continuous wave laser and a rf field. The situation is different from the CDT because the process of photon emission is dissipative and, therefore, causes decoherence in the single-molecule system. Using the renormalization group (RG) method for differential equations [6], we obtain analytical expressions for the average waiting time $\langle\tau\rangle$ of first photon emission. However, the decoherence due to finite lifetime, $1/\Gamma$, of the excited state of the molecule destroys complete localization. In other words, $\langle\tau\rangle$ is always finite. We find that $\langle\tau\rangle$ exhibits resonance behavior as a function of control parameter. The most surprising result is the existence of a critical value of Γ/ω_{rf} above which the resonance peaks (i.e., tendency to localize) disappear. The transition from coherent localizationlike behavior to noncoherent and delocalized behavior is not smooth.

We study a two-level system (a molecule) and two fields, a laser field and an electric radio frequency field. Such a system has been considered in Ref. [7]. We use the same Hamiltonian as the one used in this work; however, instead of the density matrix equation [7] we consider the Schrödinger equation with the non-Hermitian Hamiltonian, i.e., we include the relaxation term into the Hamiltonian of the system. For a molecule with a ground electronic state $|g\rangle$ and an excited electronic state $|e\rangle$, the Schrödinger equation is [3]

$$i\frac{\partial}{\partial t}|\Psi(t)\rangle = \left\{ V_g \cos\omega_{rf} t|g\rangle\langle g| + \frac{\Omega}{2}(|g\rangle\langle e| + |e\rangle\langle g|) + \left(V_e \cos\omega_{rf} t - i\frac{\Gamma}{2} + \delta\right)|e\rangle\langle e| \right\}|\Psi(t)\rangle. \quad (1)$$

Here, δ is the laser detuning, $V_{e,g}=\boldsymbol{\mu}_{e,g}\times\boldsymbol{E}_{rf}$, $\Omega=\boldsymbol{\mu}_{eg}\times\boldsymbol{E}$ (the Rabi frequency), where $\boldsymbol{\mu}_{e,g}$ are permanent dipole moments of the molecule in states $|e\rangle$ and $|g\rangle$, $\boldsymbol{\mu}_{eg}$ is the transition dipole, and $\boldsymbol{E}$ and $\boldsymbol{E}_{rf}$ stand for the amplitudes of the laser and the rf fields, respectively. In Eq. (1) we used the rotating wave approximation for the fast on-resonant laser field, but not for the slow off-resonant rf field.

The chief quantity of interest is the survival probability $P_0(t)=\langle\Psi(t)|\Psi(t)\rangle$, i.e., the probability of no emission event to occur in the time interval between 0 and t. Then, we define the average waiting time for emission event [3]

$$\langle\tau\rangle = \int_0^\infty [|\Psi_g(t)|^2 + |\Psi_e(t)|^2]dt. \quad (2)$$

In what follows, we first consider the case of $\Omega \ll \Gamma, \omega_{rf}$, and later, the case of $\Gamma < \Omega \ll \omega_{rf}$. We solve the Schrödinger equation (1) perturbatively employing the renormalization group method [6] (cf. the recent solution for CDT problem [2] with the RG procedure [8]). Note that the limit of small Rabi frequency ($\Omega \ll \omega_{rf}$) corresponds to the limit of high-frequency driving field considered previously in the CDT problem [2]. We study the effect of the non-Hermitian part of the Hamiltonian on localization behavior in the same limit.

Introducing scalings $t\mapsto\omega_{rf}t$, $V_{e,g}\mapsto V_{e,g}/\omega_{rf}$, $\delta\mapsto\delta/\omega_{rf}$, $\Gamma\mapsto\Gamma/\omega_{rf}$, $\Omega\mapsto\epsilon\Omega/\omega_{rf}$ (where $\epsilon\ll 1$), we pass to the "amplitude" variables: $\Psi_g(t)=c_g(t)\exp\{-iV_g\sin t\}$, $\Psi_e(t)=c_e(t)\exp\{-iV_e\sin t-\Gamma t/2\}$. Thus, for the case of zero detuning $\delta=0$, we arrive at the set of coupled ordinary differential equations

$$\frac{d}{dt}c_g = -i\epsilon c_e \frac{\Omega}{2}\sum_{k=-\infty}^{\infty} e^{-ikt-\Gamma t/2}J_k(\xi),$$

$$\frac{d}{dt}c_e = -i\epsilon c_g \frac{\Omega}{2}\sum_{k=-\infty}^{\infty} e^{ikt+\Gamma t/2}J_k(\xi), \tag{3}$$

where we expanded exponents in series of Bessel functions of the first kind J_k [9]

$$e^{i\xi \sin t} = \sum_{k=-\infty}^{\infty} J_k(\xi)e^{ikt}. \tag{4}$$

The modulation index $\xi = V_e - V_g$ is a parameter governing the amplitude of the driving rf field.

To solve Eqs. (3) we proceed with the application of the RG approach [6]. The naive solution to Eqs. (3) is given by a power series in small ϵ: $(c_g, c_e)^T = c^{(0)}(t) + \epsilon c^{(1)}(t) + O(\epsilon^2)$, provided that $c^{(n)}(t)$ are $O(1)$ for all t. At large enough times, however, one or several $c^{(n)}(t)$ $(n>1)$ may become greater than $c^{(0)}(t)$. Such terms, responsible for the breakdown of the naive expansion, are called secular terms. The RG procedure we carry out below regularizes the naive expansion by identifying the secular terms and eliminating them [6].

At $O(\epsilon^0)$, the solution of Eq. (3) is simply a constant vector, $c^{(0)} = (A, B)^T$. Substituting this result into the next-order equations and integrating, we have

$$c_g^{(1)} = -i\Omega B \sum_{k=-\infty}^{\infty} J_k(\xi)(1 - e^{-\Gamma t/2 - ikt})\frac{\Gamma - 2ik}{\Gamma^2 + 4k^2},$$

$$c_e^{(1)} = -i\Omega A \sum_{k=-\infty}^{\infty} J_k(\xi)(e^{\Gamma t/2 + ikt} - 1)\frac{\Gamma - 2ik}{\Gamma^2 + 4k^2}. \tag{5}$$

Further application of the naive procedure produces terms which grow with time t, i.e., secular terms

$$c_g^{(2)} = -\frac{t\Omega^2}{2}A\sum_{k=-\infty}^{\infty} J_k^2(\xi)\frac{\Gamma}{\Gamma^2 + 4k^2} + \mathcal{T}_{\mathrm{NST}},$$

$$c_e^{(2)} = -\frac{t\Omega^2}{2}B\sum_{k=-\infty}^{\infty} J_k^2(\xi)\frac{\Gamma}{\Gamma^2 + 4k^2} + \mathcal{T}_{\mathrm{NST}}, \tag{6}$$

where $\mathcal{T}_{\mathrm{NST}}$ stands for nonsecular terms. The following RG equations for variables A and B are intended to regularize the naive expansion [to order $O(\epsilon^3)$] [6]:

$$\frac{dA_R}{dt} = -\frac{\epsilon^2\Omega^2\Gamma}{2}A_R\sum_{k=-\infty}^{\infty}\frac{J_k^2(\xi)}{\Gamma^2 + 4k^2},$$

$$\frac{dB_R}{dt} = -\frac{\epsilon^2\Omega^2\Gamma}{2}B_R\sum_{k=-\infty}^{\infty}\frac{J_k^2(\xi)}{\Gamma^2 + 4k^2},$$

where subscript "R" indicates that we are solving for the renormalized values of A and B. Thus, to $O(\epsilon^3)$ A_R and B_R satisfy

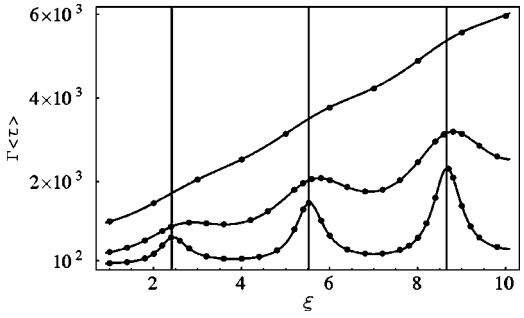

FIG. 1. Scaled mean time for the first emission $\Gamma\langle\tau\rangle$ is plotted as a function of modulation index ξ. The solid line represents RG prediction of Eq. (9); dots correspond to the numerical solution of Eq. (1). Rabi frequency $\Omega = 0.1$. Radiative decay rates are $\Gamma = 0.5$; 1.5; 3.0 (from bottom to top). Grid lines indicate zeros of $J_0(\xi)$.

$$A_R(t) = A(0)\exp\left\{-\frac{\epsilon^2\Omega^2\Gamma t}{2}\sum_{k=-\infty}^{\infty}\frac{J_k^2(\xi)}{\Gamma^2 + 4k^2}\right\},$$

$$B_R(t) = B(0)\exp\left\{-\frac{\epsilon^2\Omega^2\Gamma t}{2}\sum_{k=-\infty}^{\infty}\frac{J_k^2(\xi)}{\Gamma^2 + 4k^2}\right\}. \tag{7}$$

At time $t=0$ we assume that the molecule is in the ground state; hence, $c_e(0) = 0, c_g(0) = 1$. Applying these initial conditions and replacing A and B with their renormalized values [Eq. (7)] in $c^{(0)}$ and in Eq. (5), we obtain $O(\epsilon^2)$ perturbation results for amplitudes c_e and c_g. Then, we switch back to the original variables $\Psi_{e,g}(t)$ and arrive at [$O(\epsilon^2)$ results]

$$\Psi_g(t) = e^{-iV_g \sin t - \zeta t}, \quad \zeta = \frac{\epsilon^2\Omega^2}{2}\sum_{k=-\infty}^{\infty} J_k^2(\xi)\frac{\Gamma}{\Gamma^2 + 4k^2},$$

$$\Psi_e(t) = -i\epsilon\Omega e^{-iV_e \sin t - \Gamma t/2 - \zeta t}\sum_{k=-\infty}^{\infty} J_k(\xi) \times \frac{(e^{\Gamma t/2 + ikt} - 1)(\Gamma - 2ik)}{\Gamma^2 + 4k^2}. \tag{8}$$

For convenience we set $\epsilon = 1$, keeping in mind that the Rabi frequency Ω is small. Then, using Eqs. (2) and (8) we calculate the mean waiting time $\langle\tau\rangle$

$$\langle\tau\rangle^{-1} = \Gamma\Omega^2\sum_{k=-\infty}^{\infty}\frac{J_k^2(\xi)}{\Gamma^2 + 4k^2} + O\left(\frac{\Omega^2}{\Gamma^2}\right). \tag{9}$$

In Fig. 1 we plot the scaled mean time $\Gamma\langle\tau\rangle$, given by Eq. (9) as a function of the modulation index ξ, and compare this prediction with the results of numerical solution of Eq. (1). We observe a good agreement between the numerical and analytical results, indicating that the RG approach indeed captured the global behavior of $\Psi_{e,g}$. We also observe that, for the smallest value of the decay rate Γ (Γ/ω_{rf} in original units), maxima of $\langle\tau\rangle$ occur close to the zeros of the Bessel function $J_0(\xi)$, but with increase in Γ, the maxima of $\langle\tau\rangle$ shift and broaden.

To determine the positions of the extrema of $\langle\tau\rangle$ as a

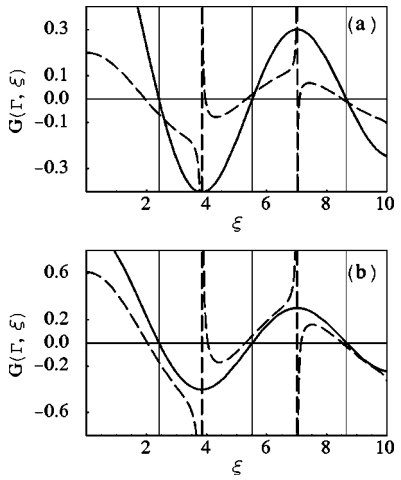

FIG. 2. Illustration of Eq. (10). Bessel function J_0 (solid line) plotted as a function of ξ together with the right-hand side of Eq. (10), $G(\Gamma,\xi)$. Radiative decay rates are (a) $\Gamma=1.0$; (b) $\Gamma=2.5$. Grid lines indicate zeros of $J_0(\xi)$.

function of ξ (Fig. 1) and to investigate the effect of the dissipation on the emission suppression (enhancement) criterion, we use Eq. (9) and set $d\langle\tau\rangle/d\xi=0$. This condition results in the following transcendental equation:

$$J_0(\xi)=\frac{\Gamma^2}{J_1(\xi)}\sum_{k=1}^{\infty}\frac{J_k(\xi)[J_{k-1}(\xi)-J_{k+1}(\xi)]}{\Gamma^2+4k^2}=G(\Gamma,\xi). \quad (10)$$

Solution of Eq. (10) yields values of ξ which minimize and maximize $\langle\tau\rangle$. These values correspond to enhancement and reduction of photon emission rate $1/\langle\tau\rangle$.

In the limit of $\Gamma\to 0$ we recover the well-known condition, obtained previously in the context of CDT, $J_0(\xi_n)=0$ (ξ_n are the zeros of the Bessel function J_0). For small Γ, since shifts in ξ with respect to ξ_n are small, we can expand both sides of Eq. (10) in Taylor series around points ξ_n. Then, the shifts of maxima are given by

$$\xi-\xi_n\sim\frac{\Gamma^2}{J_1^2(\xi_n)}\sum_{k=1}^{\infty}\frac{J_k(\xi_n)[J_{k+1}(\xi_n)-J_{k-1}(\xi_n)]}{\Gamma^2+4k^2}. \quad (11)$$

For arbitrary values of Γ, Eq. (10) has to be solved numerically. In Fig. 2 we illustrate this solution by plotting $G(\Gamma,\xi)$ and $J_0(\xi)$ versus ξ for two values of Γ. In Fig. 2(a) ($\Gamma=1.0$) we observe the graphs' crossings close to the roots of the Bessel function J_0. However, as we increase Γ to 2.5, the crossings disappear [Fig. 2(b)]. In other words, Eq. (10) does not have solutions for this value of Γ, and the first two maxima of $\langle\tau\rangle$ do not exist. A similar transition also happens with the minima of $\langle\tau\rangle$. As it follows from Eq. (10), the minima are found in the vicinity of zeros of J_1 for Γ close to zero, and disappear for sufficiently large Γ [see Fig. 2(b)].

This outcome is an indication of unexpected critical behavior of $\langle\tau\rangle$ in Γ. Maxima (minima) of the waiting time $\langle\tau\rangle$ do not disappear gradually with the increasing decay rate, due to the peaks broadening. Instead, there is a critical value of Γ for each extremum, which is equivalent to the existence

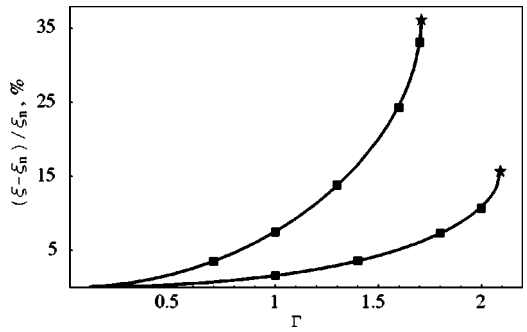

FIG. 3. The shifts $(\xi-\xi_n)/\xi_n$ found from Eq. (10) (solid lines) are compared to those found from numerical solution of Eq. (1) (boxes). They are plotted as a function of Γ (Γ/ω_{rf} in original units) for the peaks close to the first (upper curve) and the second (lower curve) zeros of J_0 (the first two peaks in Fig. 1). Critical points are marked by stars.

of an infinite number of critical points. We note that in the vicinity of critical point (ξ_{cr},Γ_{cr}), the straightforward expansion of Eq. (10) yields $\xi_{cr}-\xi\propto(\Gamma_{cr}-\Gamma)^{\beta}$, with $\beta=1/2$. Furthermore, as can be concluded from Fig. 2, the neighboring pairs of minima and maxima disappear at the same values of Γ_{cr}, that is, maxima and minima flow towards each other and annihilate. In Fig. 3 we plot shifts in the positions of maxima with respect to ξ_n given by numerical solution of Eq. (10) as a function of Γ. Both curves in Fig. 3 display excellent agreement with the results of numerical solution of the Schrödinger equation (1).

The RG procedure for the case of nonzero detuning is performed in a similar fashion and results in

$$\langle\tau\rangle^{-1}=\Gamma\Omega^2\sum_{k=-\infty}^{\infty}\frac{J_k^2(\xi)}{\Gamma^2+4(k-\delta)^2}+O\left(\frac{\Omega^2}{\Gamma^2}\right). \quad (12)$$

In this case, maxima of mean waiting time occur close to zeros of $J_\delta(\xi)$ (δ is an integer), if Γ is not large. Otherwise, they shift according to the $\delta=0$ scenario. Finally, in connection to experimental studies, we should mention that an expression $\langle\tau\rangle^{-1}$ similar to Eq. (12) was given in Ref. [10], where it adequately described the behavior of terrylene in n-hexadecane at low temperatures.

So far we have considered the situation when Rabi excitation frequency Ω is smaller than Γ. In view of single-molecule experiments carried out in Ref. [11], the opposite situation $\Omega>\Gamma$ is also important. Assuming that Ω and $\Gamma\ll\omega_{rf}$, we now turn to the criterion for the destruction of emission for this case, and verify the compatibility of the RG results and of our model Hamiltonian with the available experimental data.

Note that if Γ is smaller than ω_{rf}, we need to modify our derivation. This time, we keep the laser detuning δ in the *ee*-matrix element of the Hamiltonian in Eq. (1), and switch to "amplitudes:" $\Psi_g(t)=c_g(t)\exp\{-iV_g\sin\omega_{rf}t\}$, $\Psi_e(t)=c_e(t)\exp\{-iV_e\sin\omega_{rf}t-\Gamma t/2-i\delta t\}$. We use different scalings to ensure that the rf field frequency is much greater than both Ω and Γ (i.e., $\Gamma\mapsto\epsilon\Gamma/\omega_{rf}$, $\Omega\mapsto\epsilon\Omega/\omega_{rf}$). Our system of ordinary differential equations now reads

$$\frac{dc_g(t)}{dt} = -\frac{i\epsilon\Omega}{2}\sum_{k=-\infty}^{\infty} e^{-ikt-i\delta t}J_k(\xi)c_e(t),$$

$$\frac{dc_e(t)}{dt} = -\frac{i\epsilon\Omega}{2}\sum_{k=-\infty}^{\infty} e^{ikt+i\delta t}J_k(\xi)c_g(t) - \frac{\epsilon\Gamma}{2}c_e(t),$$

where all the quantities are in units of ω_{rf}. Unlike the previous case [Eqs. (5) and (6)], the secular terms appear (at integer values of δ) in the naive expansion already at the first order. The details of calculations with the RG method will be given elsewhere; here, we only present the final expression for the average waiting time

$$\langle\tau\rangle^{-1}(\delta) \approx \sum_k \frac{\Gamma\Omega^2 J_k(\xi)^2}{\Gamma^2 + 2\Omega^2 J_k(\xi)^2 + 4(k-\delta)^2}. \qquad (13)$$

The approximate equality sign in Eq. (13) indicates that it is only valid when resonances are not overlapping, which is consistent with our assumption $\Gamma \ll \omega_{rf}$. We see that the criterion for destruction of emission is given by $J_k(\xi)=0$ for integer values of the detuning $\delta=k$ (in units of ω_{rf}).

Now, we are ready to compare our theory with experiment of Ref. [11]. The experimental results had been matched previously with the numerical solution of optical Bloch equations [11]. We repeat the numerical simulations carried out in Ref. [11], and compare the results with analytical prediction of Eq. (13) in Fig. 4. All three graphs in Fig. 4 illustrate nearly perfect agreement between the theory and experiment. Note that generally solutions of steady-state optical Bloch equations are not identical to predictions made based on non-Hermitian Hamiltonian (which captures only the first photon statistics). However, in the limit we are considering, of small Ω and Γ, we expect good agreement (see Fig. 4).

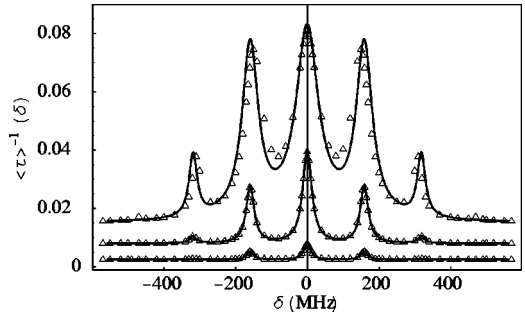

FIG. 4. Comparison of the predictions for $\langle\tau\rangle^{-1}(\delta)$ given by Eq. (13) (solid lines) with the excited state population calculated from Bloch equations (Ref. [11]) for various values of Rabi frequencies (from bottom to top): $\Omega=0.29$; 0.9; 3.2 in units of Γ. Parameters are taken from experiment of Ref. [11]: $\omega_{rf}/2\pi=140$ MHz, $\xi=1.14$, $\Gamma/2\pi=20$ MHz (empty triangles). The results are arbitrarily shifted vertically for clarity.

This work was supported by National Science Foundation Award CHE-0344930.

[1] H.-J. Stöckmann. *Quantum Chaos: An Introduction* (Cambridge University Press, Cambridge, 1999), p. 135.
[2] F. Grossmann, T. Dittrich, P. Jung, and P. Hängi, Phys. Rev. Lett. **67**, 516 (1991); M. Grifoni and P. Hängi, Phys. Rep. **304**, 229 (1998); R. Bavli and H. Metiu, Phys. Rev. Lett. **69**, 1986 (1992); M. Gitterman, J. Phys. A **34**, 10119 (2001); C. E. Creffield, Phys. Rev. B **67**, 165301 (2003).
[3] D. E. Makarov and H. Metiu, J. Chem. Phys. **115**, 5989 (2001).
[4] M. Orrit, J. Chem. Phys. **117**, 10938 (2002); E. Barkai, Y. Jung, and R. Silbey, Annu. Rev. Phys. Chem. **55**, 457 (2004).
[5] Ch. Brunel, B. Lounis, Ph. Tamarat, and M. Orrit, Phys. Rev. Lett. **83**, 2722 (1999).
[6] L. Y. Chen, N. Goldenfeld, and Y. Oono, Phys. Rev. E **54**, 376 (1996); T. Kunihiro, Prog. Theor. Phys. **97**, 179 (1997); K. Nozaki and Y. Oono, Phys. Rev. E **63**, 046101 (2001).
[7] Y. Prior and E. L. Hahn, Phys. Rev. Lett. **39**, 1329 (1977). See also Sec. V of M. B. Plenio and P. L. Knight, Rev. Mod. Phys. **70**, 101 (1998).
[8] M. Frasca, Phys. Rev. B **68**, 165315 (2003).
[9] M. Abramowitz and I. A. Stegun, *Handbook of Mathematical Functions* (Dover, New York, 1965).
[10] L. Kador, T. Latychevskaya, A. Renn, and U. Wild, J. Lumin. **86**, 189 (2000).
[11] Ch. Brunel, B. Lounis, Ph. Tamarat, and M. Orrit, Phys. Rev. Lett. **81**, 2679 (1998).